Journal of Polymer Science

WILEY

JOURNAL OF POLYMER SCIENCE

RESEARCH ARTICLE OPEN ACCESS

The Synthesis of Acrylate-Based Macromonomers and Structured Copolymers by High-Temperature Semi-Batch Radical Polymerization: The Impact of Acrylate vs. Methacrylate Monomer Choice

Elizabeth G. Bygott[1] | David Pahovnik[2] | Ema Žagar[2] | Robin A. Hutchinson[1]

[1]Department of Chemical Engineering, Queen's University, Kingston, Canada | [2]Department of Polymer Chemistry and Technology, National Institute of Chemistry, Ljubljana, Slovenia

Correspondence: Robin A. Hutchinson (robin.hutchinson@queensu.ca)

Received: 24 October 2024 | **Revised:** 12 January 2025 | **Accepted:** 6 February 2025

Funding: This work was supported by Axalta Coating Systems.

Keywords: addition-fragmentation | free-radical polymerization | macromonomer | structured copolymer

ABSTRACT

High-temperature starved-feed semi-batch radical polymerization is used to produce an isobornyl acrylate (iBoA) polymer solution with high macromonomer content without a mediating agent. The p(iBoA) macromonomer solution serves as an addition-fragmentation agent to synthesize a blocky copolymer in a single-pot sequential feeding process, as has been demonstrated using *n*-butyl acrylate (BA) as the second monomer. The impact of monomer selection on the copolymer product is investigated by switching the second monomer to *n*-butyl methacrylate (BMA) while keeping all other aspects of the operating strategy unchanged. Methodologies developed to verify macromonomer incorporation are used to compare the iBoA-BA and iBoA-BMA systems, with two-dimensional liquid chromatography providing a clear contrast between the acrylate and methacrylate (co)polymer products. The comparison demonstrates the effect of monomer structure on the macromonomer addition-fragmentation kinetics, with a blocky copolymer produced using the acrylate macromonomer only when an acrylate is used as the second monomer feed.

1 | Introduction

Polymeric dispersants are an essential additive for particle stabilization in high-performance coatings and adhesives, assisting in surface wetting and preventing the coagulation of thermodynamically unstable mixtures [1–4]. These branched or multi-block copolymers are often synthesized from polymers or oligomers with a reactive terminal double bond (TDB) unit, i.e., macromonomers [5–9]. In the presence of a second monomer, these macromonomers can be incorporated into a growing chain by radical polymerization via an addition-fragmentation cycle to form block or comb copolymers. Catalytic chain transfer (CCT) with a cobalt complex among other controlled radical techniques efficiently produces methacrylate-based macromonomer solutions [10–15]. However, CCT yields low TDB content when applied to acrylate and styrenic systems [16–18]. While acrylate macromonomer solutions have been synthesized using other strategies [9, 19–23], the use of a mediating agent and/or the need for low polymer contents limit process efficiency and make scale-up difficult [24].

Our group has recently demonstrated the ability to efficiently produce acrylate macromonomers without a mediating agent under the high-temperature starved-feed semi-batch operating policies used commercially to produce acrylate-methacrylate-styrene acrylic resins in solution [25–27] with high polymer

contents and low molar masses at low initiator levels [28–32]. Reactant feeding ensures tight control of polymer composition and near-isothermal operation, both of which are difficult to achieve under batch conditions [24, 28]. Moreover, the high temperatures and low monomer concentrations increase the importance of acrylate side reactions (Figure S1), including backbiting and macromonomer production via β-scission [25–29, 32–36]. The operating strategy was first used to homopolymerize *n*-butyl acrylate (BA) at 140°C and 160°C over a range of monomer and initiator levels [27]. When operating at high polymer contents (65 wt.%), a maximum TDB content of ~50% was obtained with 0.5 mol% initiator relative to the monomer in the feed [25, 27]. Higher TDB fractions could not be reached due to the reaction of the macromonomers with other radicals in the system via an addition-fragmentation cycle (Figure S1b) that consumed TDBs and increased polymer molar masses via macromonomer incorporation (i.e., branching) [25–27, 36]. However, when the acrylate monomer was switched to isobornyl acrylate (iBoA), a significantly higher TDB content was obtained under identical operating conditions, > 80% at 160°C [25]. This difference was explained by steric hindrance provided by the bulky isobornyl ester group that favors mid-chain radical (MCR) fragmentation (i.e., TDB formation) over monomer addition (i.e., TDB consumption and branch formation), thereby increasing the p(iBoA) TDB content and decreasing polymer branching and dispersity ($Đ$) [25, 26].

The differing relative addition and fragmentation rates found for BA and iBoA led to the development of a single-pot semi-batch sequential feeding process to produce blocky copolymers by radical polymerization without a mediating agent [25, 26]. A high TDB content p(iBoA) macromonomer solution is first produced through the starved-feed addition of iBoA and initiator to a solvent-charged reactor, with the feed then switched to the second monomer (while maintaining initiator addition) halfway through the process; the p(iBoA) macromonomers are incorporated into the growing chains of the second monomer via the addition-fragmentation cycle to yield blocky copolymer structures. As schematically outlined in Figure 1a, the sequence starts with p(iBoA) macromonomer addition to a monomer-2 growing chain to produce an MCR. β-Scission of the MCR either re-forms the original p(iBoA) macromonomer and radical or occurs in the other direction to form a monomer-2 chain with an iBoA TDB and a propagating p(iBoA) radical that, through subsequent monomer-2 addition (pathway 1), forms a block copolymer chain. Competing with fragmentation is the addition of monomer-2 to the MCR (pathway 2) to produce a comb copolymer chain containing an iBoA branch, reducing the TDB content in the system. This approach is also shown mechanistically for an acrylate-acrylate system in Figure S2 of the Supporting Information.

The addition-fragmentation events outlined in Figure 1a can occur with any macromonomer and/or radical species in the system, resulting in several pathways to form multiblock linear or branched structures. For example, a propagating block copolymer radical can react with any macromonomer (homopolymer or copolymer) in the system, increasing the number of blocks in

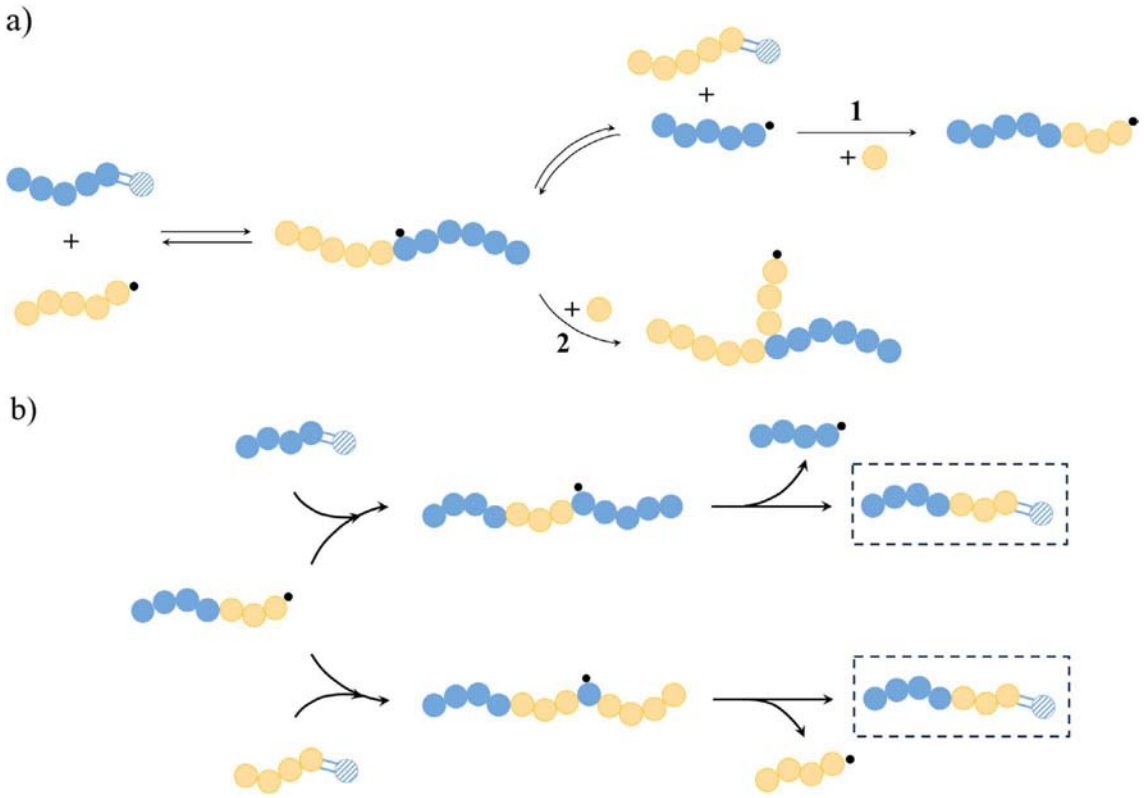

FIGURE 1 | Schematics illustrating: (a) the addition-fragmentation pathways to produce block (1) and comb (2) copolymers by feeding a second monomer (yellow) into the reactor containing p(iBoA) macromonomer chains (blue, with the terminal double bond indicated by the striped unit); (b) two of many potential β-scission pathways to form macromonomer-terminated copolymer chains (boxed structure) capable of further reaction to form multi-block linear or branched structures.

the chain via β-scission of the resultant MCR, as illustrated by Figure 1b, or adding more branch points to the comb structure by monomer addition to the MCR. Moreover, it is necessary to consider that growing blocky acrylate copolymer radicals can backbite and undergo subsequent β-scission or monomer addition. While our focus is on the formation and utilization of acrylate-based macromonomers, Heuts and Smeets [37], and Nurumbetov et al. [38] also describe these mechanisms for acrylate polymerization in the presence of a methacrylate-based macromonomer.

Our previous work demonstrated the ability of the novel one-pot operating strategy to efficiently synthesize acrylate-acrylate blocky copolymers under a range of operating conditions, with BA selected as the second monomer. The incorporation of the p(iBoA) macromonomer was verified by various techniques, including detailed analysis of the evolution of the product molar mass distributions (MMDs), electrospray ionization mass spectroscopy (ESI-MS), and polymer fractionation followed by TDB, composition, and molar mass analysis [25].

Not yet investigated is the choice of second-stage monomer, which is expected to greatly impact the polymer structure as controlled by the addition-fragmentation pathway. The literature indicates only a minor influence of ester group functionality on acrylate mechanistic pathways [26]. However, switching the second monomer to a methacrylate will affect both the comonomer incorporation and structure of the product [6, 25, 27, 37–40]. Herein, we investigate the impact of using *n*-butyl methacrylate (BMA) as the second-stage monomer rather than BA, keeping all other aspects of the process unchanged. The previously developed analytical methodologies are used to compare the iBoA-BA and iBoA-BMA systems, with two-dimensional liquid chromatography (2D-LC) analysis providing additional insights.

2 | Results and Discussion

The sequential monomer feeding methodology described in our previous study [25] is used to examine the influence of switching the second monomer feed from an acrylate (BA) to a methacrylate (BMA). iBoA was first fed at a constant rate to a solvent-charged reactor maintained at 140°C for 1.5 h to produce the p(iBoA) macromonomer, followed by 1.5 h of BA (or BMA) feed. The initiator was fed at 0.5 mol% relative to the monomer to achieve a final polymer content of 65 wt.% in 5-methyl-2-hexanone (MIAK) and a composition of 50 wt.% iBoA assuming full monomer conversion. The iBoA conversion was ~85% when starting the second monomer feed such that the quantity of random copolymer produced was negligible. The evolution of the MMDs with reaction time for each experiment after the initial p(iBoA) formation (MMD at 90 min) is shown in Figure 2.

The p(iBoA) MMD remains narrow over the 90-min iBoA feed, reaching a weight-average molar mass (M_w) of just over 5000 g•mol^{-1} while maintaining a TDB content >70%. As described previously [25], this result is characteristic of high levels of β-scission and minimal incorporation of the resulting macromonomer into the growing p(iBoA) chains to form branches. Herein, we focus on the second monomer feed and the impact of adding BMA rather than BA to the p(iBoA) macromonomer solution.

For the first case, where the monomer feed was switched from iBoA to BA at 90 min, the MMD (Figure 2a) broadened and developed a bimodality as it shifted to higher molar masses, reaching a final M_w of 12,700 g•mol^{-1} and a $Đ$ of 2.18. In addition to the increasing M_w and $Đ$, the position of the MMD peak shifts to higher values over the course of the BA feed while the TDB content decreases (Table 1), indicating that the p(iBoA) macromonomers are incorporated into the growing p(BA) chains to form predominately comb copolymers [25]. To test the impact of acrylate structure on the predominant mechanistic pathway, the experiment was repeated with a mixture of 25 wt.% 2-hydroxyethyl acrylate (HEA) and 75 wt.% BA in the second monomer feed. Similar to the 100% BA case, the MMD (Figure S3) shifted to a final M_w of 13,000 g•mol^{-1} and a $Đ$ of 2.23. The minor impact of adding HEA to the second stage suggests that acrylate functionality has little mechanistic impact, consistent with the family-type behavior observed with acrylate monomers.

Repeating the sequential feed experiment using BMA rather than BA also results in a broadening of the MMD (Figure 2b) and an increase in molar mass to a final M_w of 15,900 g•mol^{-1} and $Đ$ of 3.42. Unlike the BA case, however, the peak position of the MMD stays constant as BMA is fed, with a second peak

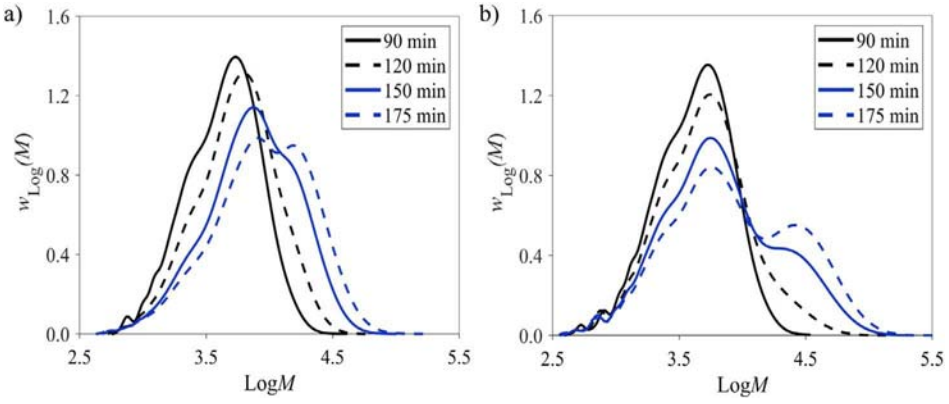

FIGURE 2 | The evolution of the polymer MMD for sequential monomer feeding with a 90-min iBoA feed followed by a 90-min feed of (a) BA or (b) BMA. Both experiments were conducted to 65 wt.% final polymer/monomer content in MIAK at 140°C with a feed containing 0.5 mol% initiator relative to monomer. The evolution of polymer properties with time is reported in Table 1.

TABLE 1 | Evolution of polymer characteristics for semi-batch operation with a 90-min iBoA feed followed by a 90-min BA or BMA feed to 65 wt.% final polymer/monomer content at 140°C with a feed containing 0.5 mol% initiator relative to monomer.

	iBoA-*block*-BA				iBoA-*block*-BMA			
Time[a] [min]	M_w [g•mol^{-1}]	$Đ$ [–]	*U%* [%]	*TDB%* [%]	M_w [g•mol^{-1}]	$Đ$ [–]	*U%* [%]	*TDB%* [%]
90	5300	1.54	4.5	75 ± 3	5100	1.58	4.7	72 ± 3
120	7100	1.69	3.0	68 ± 2	7200	2.00	3.8	69 ± 3
150	10,000	1.94	1.9	58 ± 2	11,900	2.85	2.8	64 ± 2
175	12,700	2.18	1.3	49 ± 1	15,900	3.42	2.3	60 ± 2

[a]Polymer weight-average molar mass (M_w) and dispersity ($Đ$) measured by size-exclusion chromatography with refractive index detection. The number of macromonomer end groups relative to the number of repeat units in the polymer (*U%*) is calculated using proton nuclear magnetic resonance spectroscopy, with the fraction of chains containing a terminal double bond (*TDB%*) calculated as the product of the *U%* and number average degree of polymerization.

at a higher molar mass gradually emerging. This result suggests that the product consists predominantly of a mixture of two homopolymers, lower molar mass p(iBoA) and higher molar mass p(BMA). The striking difference between the two systems is even clearer when the MMDs are scaled according to the weight fraction of iBoA in the final polymer (Figure S4). The BA case shows a loss of the low p(iBoA) molar mass material relative to that present after the iBoA homopolymerization stage, indicating that the macromonomer chains have been incorporated into the product. In contrast, there is negligible reduction of the scaled 90-min p(iBoA) peak when BMA is added as the second monomer. The significant differences between the two systems can also be seen after transforming the SEC $w_{\log}(M)$ MMDs to number chain length distributions. While a loss of p(iBoA) chains is seen when BA is fed, there is a marginal loss of p(iBoA) chains with BMA as the second monomer (Figure S5).

In our previous study, the decrease in TDB content in the all-acrylate system was used to assess the incorporation of the p(iBoA) macromonomer into the growing BA chains to produce a branched product, as the backbiting and β-scission mechanisms occur in both monomer systems [25–27, 29, 41–44]. However, when the second-stage monomer is switched to a methacrylate, the decrease in TDB content can no longer be used to assess macromonomer incorporation into the growing polymer chains. Unlike acrylates, methacrylates do not undergo backbiting or β-scission, with unsaturated chains only formed through radical-radical termination by disproportionation [28, 32, 45–47], resulting in lowered TDB levels for p(BMA) semi-batch homopolymerizations compared to acrylate systems (Table S2). Thus, the decrease in TDB content for the product formed by sequential iBoA and BMA feeding (Table 1) is attributed to the dilution of the p(iBoA) macromonomer population by the formation of saturated p(BMA) chains, rather than by the incorporation of the macromonomer into a comb copolymer product.

In addition to the final distribution and TDB content, the difference in the polymer compositions when switching from BA to BMA is worth noting. The final polymer contains 49 wt.% p(BA) for the BA case, whereas the p(BMA) fraction is only 39 wt.% under identical operating conditions. This difference can be attributed to the depropagation of BMA at high temperatures and the low monomer concentrations used in semi-batch starved feed operations [28, 45, 46]. This is evident by the decreased final conversion for BMA (57%) relative to BA (86%), and an increased residual monomer fraction (Figure S6).

Our previous work introduced a precipitation-centrifugation technique using methanol to fractionate the polymer product into high and low molar mass components to evaluate macromonomer incorporation [25]. When applied to the homopolymer iBoA macromonomer, the methanol soluble and insoluble fractions have approximately the same TDB content, indicating uniform TDB levels across the MMD [25]; electrospray ionization mass spectroscopy (ESI-MS) analysis indicated that the most abundant chain structure in each p(iBoA) fraction is β-scission radical-initiated and macromonomer terminated, as mechanistically shown in Figure S1a [25]. When applied to the p(iBoA-*block*-BA) product, the methanol insoluble fraction contained a reduced TDB and BA content compared to the unfractionated material. Moreover, the p(iBoA) macromonomer chains disappeared from the ESI-MS analysis of the p(iBoA-*block*-BA) product, indicating that they were incorporated into the growing BA chains to form a blocky copolymer of higher molar mass [25].

The precipitation-centrifugation technique has been applied to the final sample of the sequential feed experiment with BMA to contrast the ESI-MS results with our previous work. The insoluble and soluble fractions of the copolymer were also analyzed by SEC and proton nuclear magnetic resonance (^{1}H NMR) spectroscopy, with results summarized in Figure S7 and Table S3. As shown in Figure 3, the predominant structure in the low molar mass region ($\leq$3000 g•mol^{-1}) of the insoluble fraction remains the p(iBoA) macromonomers, indicating that they are not incorporated into the chains formed during polymerization of the BMA. Figure S8 in the Supporting Information presents the ESI-MS results of a second molar mass region, with specific chain structures assigned according to the initiating and terminating species summarized in Table S4. While there is some indication of copolymer formation from ESI-MS analysis of the methanol-soluble fraction, the continued presence of unreacted p(iBoA) macromonomer confirms that using BMA rather than BA limits the formation of a blocky copolymer product.

The differences in p(iBoA) macromonomer incorporation into the p(BA) or p(BMA) growing chains are evident when applying the previously developed analyses to compare product TDB contents and MMDs. The structure of the resultant products

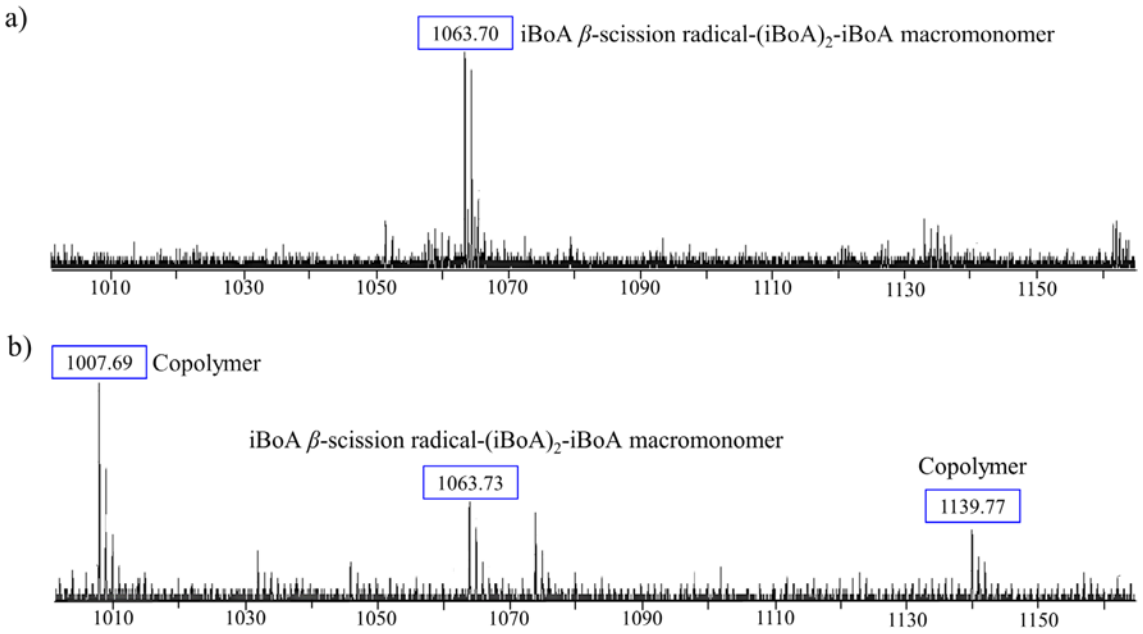

FIGURE 3 | The electrospray ionization mass spectroscopy spectrum of the methanol (a) insoluble and (b) soluble fractions of the 50/50 iBoA/BMA sequential feed experiment for the m/z region of 1000 to 1160 g•mol^{-1}. See Table S4 for the initiating and terminating species associated with specific chain structures.

was further evaluated using two-dimensional liquid chromatography (2D-LC). As detailed in the experimental section, the fully-automated set-up uses reverse-phase liquid adsorption chromatography (RP-LAC) to first separate the polymer sample according to its chemical composition, followed by SEC in the second dimension to separate the fractions from the first dimension according to their hydrodynamic volume to obtain a fingerprint of the (co)polymer structure. This technique was used by Zdovc et al. [48] to contrast structured block and gradient copolymers and by Alshehri et al. [49] to study gradient iBoA-BA copolymers produced by reversible-addition-fragmentation chain transfer (RAFT) emulsion polymerization.

Before conducting the 2D-LC experiments, RP-LAC was used to compare p(iBoA), p(BA), and p(BMA) homopolymers of varying molar masses, and to analyze the block and random copolymers according to their chemical composition, with the 50/50 wt.% iBoA/BA random copolymer produced as a comparison to the blocky case by feeding a 50/50 w/w mixture of the two monomers over 3 h in the semi-batch system to 65 wt.% solids at 140°C. As shown in Figures 4a and 5a, the more polar BA and BMA chains eluted at approximately 7.4 mL and 7.7 mL respectively, whereas the less polar iBoA polymer eluted at 9.2 mL. The p(BA) and p(BMA) eluted with relatively narrow peaks and demonstrated little molar mass dependence for the operating range, whereas the broader p(iBoA) peaks and molar mass dependence indicated greater interactions with the column. Despite the low molar mass operating range required for the copolymers, the RP-LAC and 2D-LC results can be used to qualitatively assess macromonomer incorporation and copolymer composition across the MMD.

The RP-LAC peak is wider and closer to the expected p(iBoA) elution volume for the iBoA-BA sequential feed blocky copolymer product than the random copolymer (Figure 4a). While composition has the dominant influence on elution volume, the two samples both contain 50 wt.% iBoA. Thus, the difference arises from the change in copolymer microstructure; the probability of the iBoA segments interacting with the stationary phase is increased when switching from a statistical to a block copolymer, slowing the elution and increasing the width of the peak [48]. Moreover, the breadth and tailing of this peak, centered at 8.8 mL between the positions of the random copolymer and p(iBoA) peaks, also suggests that the p(iBoA) blocks in the copolymer chains are dispersed in length, as might be expected from the stochastic nature of the radical polymerization synthesis process (Figure 1b). This observation is consistent with the work of Zdovc et al., who obtained a narrower peak than that observed in Figure 4a for a block copolymer with close to monodisperse block lengths [48].

The corresponding 2D-LC plot (Figure 4b) indicates that the blocky (iBoA-BA) copolymer chains are the most abundant material in the final product. The molar mass of this copolymer product is significantly higher than that of the less abundant p(BA) and p(iBoA) homopolymer material, with the p(iBoA) homopolymer likely a combination of non-macromonomer terminated and unincorporated macromonomer chains. In contrast, the 2D-LC plot for the random copolymer has a uniform composition across the MMD (Figure S9). Thus, the RP-LAC and 2D-LC analyses confirm that most growing p(BA) chains incorporate at least one p(iBoA) macromonomer into their structure with the sequential feed operating strategy.

The 2D-LC results for the iBoA-BMA sequential feed experiment provide a strong contrast to the iBoA-BA case. The RP-LAC analysis of the material produced with BMA as the second monomer (Figure 5a) indicates that the feeding strategy produces predominantly a mixture of two homopolymers with little copolymer, as the two peaks seen in the RP-LAC chromatogram of the product trace occur at the same elution volume range as those of the

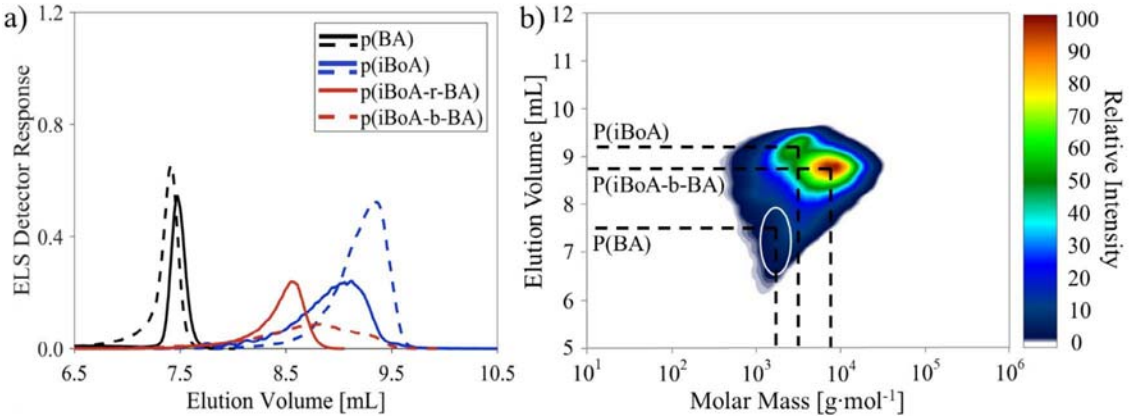

FIGURE 4 | (a) The reverse-phase liquid adsorption (RP-LAC) chromatograms for p(BA) and p(iBoA) homopolymers of two different molar masses, a 50/50 statistical copolymer, and a blocky copolymer formed by sequential monomer feeding. The molar masses of the two samples analyzed for each homopolymer as indicated by the solid and dashed lines are summarized in Table S5. (b) The 2D-liquid chromatography contour plot for polymer formed by sequential feeding of iBoA and BA in the semi-batch process. The first dimension (*y*-axis) is RP-LAC and the second (*x*-axis) is SEC with the molar mass in polystyrene equivalents. The color scale is the relative intensity of material by evaporative light scattering (ELS) detection.

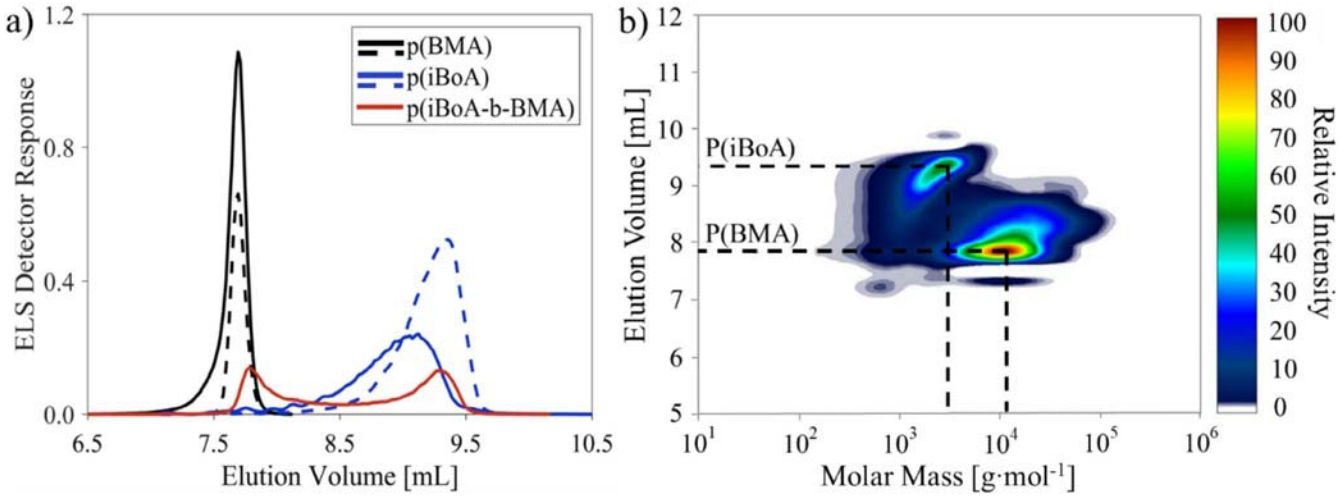

FIGURE 5 | (a) The reverse-phase liquid adsorption (RP-LAC) chromatograms for p(BMA) and p(iBoA) homopolymers of two different molar masses and the corresponding blocky copolymer. The molar masses of the two samples analyzed for each homopolymer as indicated by the solid and dashed lines are summarized in Table S5. (b) The 2D-liquid chromatography contour plot for polymer formed by sequential feeding of iBoA and BMA in the semi-batch process. The first dimension (*y*-axis) is RP-LAC, and the second (*x*-axis) is SEC with the molar mass in polystyrene equivalents. The color scale is the relative intensity of the evaporative light scattering (ELS) detector.

corresponding homopolymer controls. The 2D-LC plot (Figure 5b) shows that the p(BMA) homopolymer is the most abundant material in the product, followed by unreacted p(iBoA) material, and that only low quantities of copolymer chains were formed that eluted in the RP-LAC dimension (*y*-axis) between the elution volumes of the two homopolymers. The contour plot also confirms that the higher molar mass peak in the final MMD (Figure 2b) is primarily p(BMA), while the lower molar mass peak is the unreacted p(iBoA) macromonomer. Therefore, consistent with the inferences made by the other characterizations, RP-LAC and 2D-LC analyses conclusively indicate that the growing p(BMA) chains rarely incorporate a p(iBoA) macromonomer, resulting in a mixture of two homopolymers in the final product.

The RP-LAC and 2D-LC results support the interpretation that the acrylate-acrylate sequential feed experiment with 50/50 iBoA/BA produces a blocky comb copolymer, but when the second monomer feed is switched to BMA, homopolymerization is favored. Studies in the literature have determined that the polymerization behavior of TDBs is dependent upon the identity of the penultimate unit of the macromonomer and the second-stage polymerization conditions [6, 25, 27, 37–39]. The addition of an acrylate macromonomer to a methacrylate radical (i.e., as produced by our iBoA-BMA sequential feed) and the addition of a methacrylate macromonomer to an acrylate radical (as considered by Heuts and Smeets [37]) both result in an MCR structure as shown in Figure 6; that is, one that is flanked by both an adjacent methacrylate unit and an adjacent acrylate unit. Fragmentation is favored to transfer the radical to the methacrylate, due to the added stabilization of the methyl group [39]. This leads to block copolymer formation for acrylate polymerization in the presence of a methacrylate macromonomer, as shown by

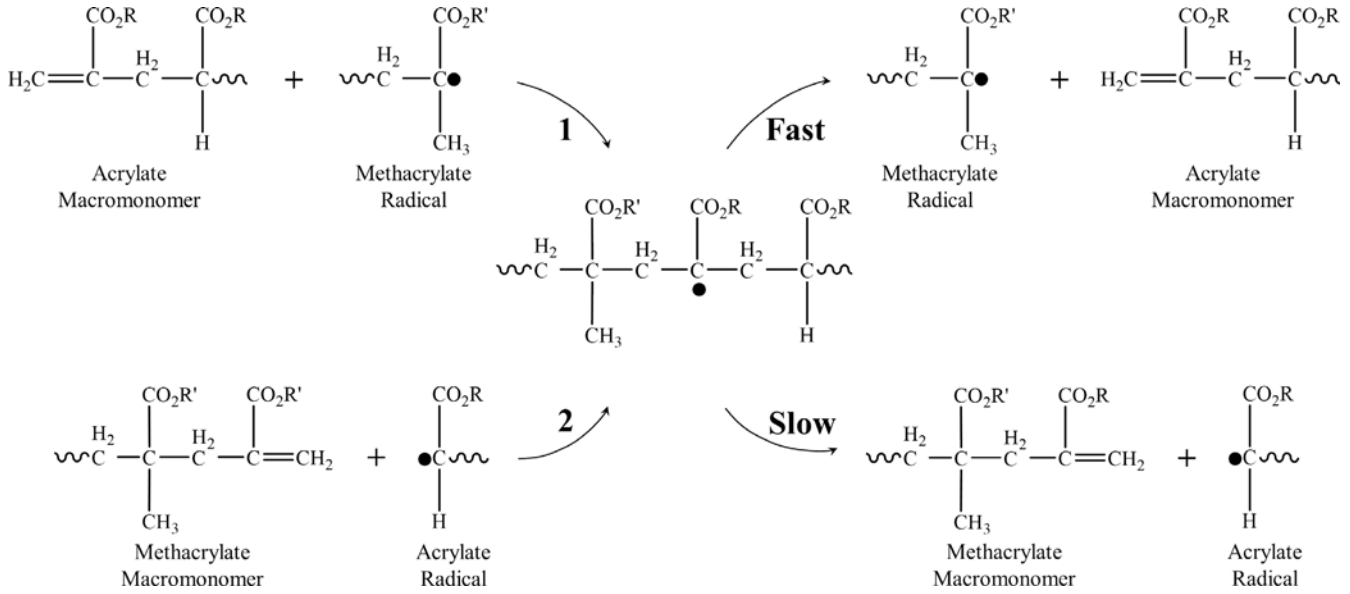

FIGURE 6 | β-Scission pathways for the mid-chain radical (MCR) formed by either the addition of an acrylate macromonomer to a methacrylate radical (1) or the addition of a methacrylate macromonomer to an acrylate radical (2).

Yamada and coworkers [6, 39]. However, the favored fragmentation pathway means that minimal block copolymer formation occurs when acrylate macromonomer is added to a methacrylate polymerization; instead, the MCR fragments back to the original methacrylate radical and acrylate macromonomer reactants. This second scenario describes the iBoA-BMA sequential feed experiment studied here, with the MMD, ESI-MS, and 2D-LC analyses all confirming that the product is predominantly a mixture of two homopolymers.

3 | Conclusion

High-temperature starved-feed semi-batch radical polymerization of iBoA is an effective means to produce high macromonomer content solutions without a mediating agent, thus providing a means to synthesize blocky copolymers by sequential feeding of iBoA and a second acrylate monomer. In this work, we test the impact of changing the second-stage monomer from acrylate BA to methacrylate BMA, under otherwise identical operating conditions. BMA addition to the p(iBoA) macromonomer solution results in a minimal decrease in polymer TDB content and a broadening of the MMD due to the gradual formation of a high molar mass peak, suggesting that, in contrast to the iBoA-BA case, the product is primarily a mixture of two homopolymers. This result was confirmed by fractionating the product into two components that were also analyzed by SEC, ^{1}H NMR, and ESI-MS. The 2D-LC analysis provided the final evidence that, while blocky copolymer is the most abundant product formed from the iBoA-BA sequential feed procedure, a mixture of primarily two homopolymers is obtained when the second monomer feed is switched to BMA. Thus, it can be concluded that the MCR formed by the addition of the growing methacrylate radical to the acrylate macromonomer preferentially fragments back to the original methacrylate radical and acrylate macromonomer. Further work will focus on the successful acrylate-acrylate sequential feed process, quantifying the amount of homopolymer impurity in the blocky copolymer product.

4 | Experimental

4.1 | Materials

n-Butyl acrylate (10–60 ppm monomethyl ether hydroquinone as an inhibitor, ≥99%, Sigma-Aldrich), isobornyl acrylate (200 ppm monomethyl ether hydroquinone as an inhibitor, technical grade, Sigma-Aldrich), 2-hydroxyethyl acrylate (200–650 ppm monomethyl ether hydroquinone as inhibitor, 96%, Sigma-Aldrich), and *n*-butyl methacrylate (8–28 ppm monomethyl ether hydroquinone as an inhibitor, ≥98.5%, Sigma-Aldrich) monomers were used as received to match common industrial practice unless otherwise stated. *tert*-Butyl peracetate initiator (TBPA, 50 wt.% in mineral spirits, Sigma-Aldrich), 5-methyl-2-hexanone (MIAK, 99%, Sigma-Aldrich), tetrahydrofuran (THF, Sigma-Aldrich), methanol (ACS reagent grade, Sigma-Aldrich), hydroquinone (MEHQ, ≥99%, Fluka), and chloroform-D ($CDCl_3$, 99.8 D, Sigma-Aldrich) were used as received at Queen's University. Tetrahydrofuran (Optima, Fisher Chemical), methanol (Optima LC/MS, Fisher Chemical), acetonitrile (Optima LC/MS, Thermo Scientific), and sodium iodide (99.999% trace metals basis, Sigma-Aldrich) were used as received for ESI-MS at Axalta Coating Systems. Tetrahydrofuran (≥99.9%, Riedel de Haën, Germany), and acetonitrile (≥99.9%, Riedel de Haën, Germany) were used as received for RP-LAC and 2D-LC at the National Institute of Chemistry.

4.2 | Polymer Synthesis

Starved-feed semi-batch polymerizations were conducted using a 1-L double-walled glass LabMax reactor with an agitator and reflux condenser. Camile TG software controlled the reaction temperature, mixing, and feed rates. The reactor was initially charged with 130 g of MIAK and heated to the reaction temperature of 140°C under a nitrogen blanket. 121 g of TPBA and iBoA were fed for 90 min followed by a 90 min feed of 121 g of either BA/TBPA, BA/HEA/TBPA, or BMA/TBPA.

The monomer/initiator mixtures, containing 0.5 mol% initiator relative to monomer, were fed at a constant flow rate over the total reaction time of 3 h to a final polymer/monomer content in solution of 65 wt.%. Samples of approximately 3 mL were taken from the reactor at specified times and placed into a solution of MEHQ in solvent (1 g•L^{-1}) to terminate the reaction. Note that the BA, BMA, and iBoA homopolymers and the iBoA/BA random copolymer used for the 2D-LC analysis were produced using the same operating strategy with a 3 h feed time.

4.3 | Characterization Techniques

A Varian CP-3800 gas chromatograph (GC) with a CP-8410 auto-sampler, CP-117 isothermal split/splitless injector, Rtx-5 fused silica column (length 30 m, i.d. 0.25 mm, film thickness 1.0 μm), and a flame ionized detector (FID) was used to estimate the residual monomer weight fractions and thus copolymer compositions in the samples relative to calibrations generated using mixtures of known composition. The instrument was operated with an injector flow rate of 1.2 mL•min^{-1}, an inlet temperature of 275°C, and an FID temperature of 300°C. Ultrahigh-purity hydrogen and zero-grade compressed air were used as combustion gases, and ultrahigh-purity helium and nitrogen were used as carrier gases under a constant pressure of 16.4 psi. Samples were diluted in THF by a factor of 10 relative to the starting volume before injection.

SEC was conducted using a Waters 2960 separation module with a Waters 410 differential refractometer and Waters Styragel high-resolution separation columns (4.6 × 300 mm) 0.5, 1, 3, 4. The instrument was operated at 40°C with a THF flow rate of 0.3 mL• min^{-1}. Samples were dried under air, dissolved in THF, and passed through a 0.22 μm nylon filter before injection. The molar mass outputs were processed based on a calibration curve constructed using narrow molar mass polystyrene standards ranging from 370–860,000 g•mol^{-1}. Mark-Houwink parameters were used to transform the polymer MMDs and corresponding characteristics from polystyrene equivalents (Table S1), with copolymer values estimated using a composition-average approach.

It should be noted that using SEC analysis to determine true M_w and M_n values for block copolymer structures can be complicated by the influence of block length and monomer choice on chain solubility and conformation [50]. While the use of a copolymer-composition weighted approach can introduce error, we expect that it is small based on two observations: (i) MMDs measured by multi-angle light scattering show good agreement with those estimated by RI detection [25, 26]; (ii) the low molar mass and multiblock structure of our copolymer chains does not lead to distinct phase transitions (e.g., two glass transition temperatures). The error introduced by using a composition-averaged calibration is likely increased for the iBoA/BMA system, as the product consists primarily of a mixture of two homopolymers; however, the conclusions regarding the extent of macromonomer incorporation remain unchanged.

^{1}H NMR was conducted using a 500 MHz Bruker Avance NEO spectrometer at room temperature with 64 scans. The samples were prepared by evaporating the reaction solvent and residual monomer(s) under air and dissolving the polymer in $CDCl_3$ to approximately 10 wt.% polymer. The resulting spectrum was used to estimate the *U*%, following procedures developed in our previous work [25]. The *U*% was combined with the DP_n determined by SEC analysis to estimate the percentage of chains that contain a TDB [25–27].

The methanol soluble and insoluble fractions obtained from the precipitation-centrifugation technique were analyzed by ESI-MS using a Waters SYNAPT high-definition mass spectrometer in the positive ionization mode for a mass range of 50–4000 g•mol^{-1}. Samples were prepared by dissolving the polymer in unstabilized Optima grade THF to 1 mg•mL^{-1}, further diluting to 50 μg•mL^{-1} in ACN, and adding 3 μL of sodium iodide solution (10 μg•mL^{-1} in Optima grade methanol). Scans were acquired using a sampling cone voltage of 40 V, a capillary voltage of 3.5 kV, a source temperature of 80°C, a desolvation temperature of 150°C, and a sample infusion rate of 5 μL•min^{-1}. Initiating and terminating species are summarized in Table S4 of the supporting Information.

RP-LAC experiments were performed on a reversed-phase Zorbax Eclipse Plus C18 column (4.6 mm × 150 mm, 95 Å, 5 μm, Agilent Technologies, USA) at 25°C maintained by thermostatted oven. Samples were dissolved in a 50/50 vol% ACN/THF mixture at a concentration of 1 mg•mL^{-1} and stirred overnight. The solvent gradient ran from 0% to 100% THF in ACN in 10 min. The flow rate during the analysis was 1 mL•min^{-1}, and the injected volume of the samples was 20 μL. Two detectors connected in series were used, an ultraviolet (UV) detector operating at a wavelength of 280 nm and an evaporative light scattering (ELS) 1260 Infinity detector, both from Agilent Technologies. The ELS detector was operated under the following conditions: T_{evap} = 70°C; T_{neb} = 40°C and a nitrogen flow rate of 1.60 SLM. WinGPC v.8 software (Polymer Standards Service GmbH, Germany) was used for data acquisition and analysis.

For 2D-LC analyses, a Zorbax Eclipse Plus C18 column (4.6 mm × 150 mm, 95 Å, 5 μm, Agilent Technologies, USA) and an SDV-linear M high-speed, linear porosity SEC column (20 mm × 50 mm I.D., particle size 5 μm, Polymer Standards Service, PSS GmbH, Germany) was used. In the first RP-LAC dimension, the flow rate was 0.025 mL min^{-1} and the solvent gradient ran from 0% to 100% THF in ACN in 400 min. Samples were dissolved in a 50/50 vol% ACN/THF mixture at a concentration of 10 mg•mL^{-1} and stirred overnight. The injected volume of the copolymer samples was 20 μL. THF was the mobile phase in the second SEC dimension, with the flow rate set to 3 mL•min^{-1}. The high-speed SDV column has a broad pore size distribution covering molar masses from 10^2 to 10^6 g•mol^{-1}. The SEC column was calibrated with eight polystyrene (PS) standards with narrow MMDs dissolved in THF at a concentration of 0.5 mg•mL^{-1} and injected directly into the second dimension at a flow rate of 3.0 mL•min^{-1}. The fractions were transferred from the first to the second dimension via an eight-port valve (Valco Instruments) equipped with two 200 μL sample loops. The same detectors and software were used for detection and data acquisition as in the RP-LAC section.

Acknowledgments

The authors acknowledge Axalta Coating Systems and Dr. Michael Grady for consultation and financial support and Axalta for completing the electrospray ionization mass spectroscopy analyses. Dr. Blaž Zdovc is gratefully acknowledged for his help with 2D-LC analyses.

References

1. C. Auschra, E. Eckstein, A. Mühlebach, M.-O. Zink, and F. Rime, "Design of New Pigment Dispersants by Controlled Radical Polymerization," *Progress in Organic Coating* 45 (2002): 83–93.

2. J. Bieleman, W. Heilen, S. Silber, M. Ortelt, and W. Scholz, *Additives for Coatings*, J. Bieleman (Wiley-VCH, 2000).

3. S. Q. A. Rizvi, *Surfactants and Detergents: Chemistry and Applications* (ASTM International, 2021).

4. J. A. Simms, "A New Graft Polymer Pigment Dispersant Synthesis," *Progress in Organic Coating* 35 (1999): 205–214.

5. Y. Yamashita, K. Ito, H. Mizuno, and K. Okada, "Synthesis of Amphiphilic Graftcopolymers From Polystyrene Macromonomer," *Polymer Journal* 14 (1982): 255–260.

6. B. Yamada, P. Zetterlund, and E. Sato, "Utility of Propenyl Groups in Free Radical Polymerization: Effects of Steric Hindrance on Formation and Reaction Behavior as Versatile Intermediates," *Progress in Polymer Science* 31 (2006): 835–877.

7. S. Ohno and K. Matyjaszewski, "Controlling Grafting Density and Side Chain Length in Poly(*n*-butyl acrylate) by ATRP Copolymerization of Macromonomers," *Journal of Polymer Science, Part A: Polymer Chemistry* 44 (2006): 5454–5467.

8. J. Krstina, C. L. Moad, G. Moad, E. Rizzardo, C. T. Berge, and M. Fryd, "A New Form of Controlled Growth Free Radical Polymerization," *Macromolecular Symposia* 111 (1996): 13–23.

9. J. Chiefari, J. Jeffery, R. T. A. Mayadunne, G. Moad, E. Rizzardo, and S. H. Thang, "Chain Transfer to Polymer: A Convenient Route to Macromonomers," *Macromolecules* 32 (1999): 7700–7702.

10. D. M. Haddleton, D. R. Maloney, and K. G. Suddaby, "Competition Between β-Scission of Macromonomer-Ended Radicals and Chain Transfer to Cobalt(II) in Catalytic Chain Transfer Polymerization (CCTP)," *Macromolecules* 29 (1996): 481–483.

11. D. M. Haddleton, D. R. Maloney, K. G. Suddaby, A. Clarke, and S. N. Richards, "Radical-addition-fragmentation and Co-polymerization of Methyl Methacrylate Macromonomers from Catalytic Chain Transfer Polymerization (CCTP)," *Polymer* 38 (1997): 6207–6217.

12. J. P. A. Heuts, G. E. Roberts, and J. D. Biasutti, "Catalytic Chain Transfer Polymerization: An Overview," *Australian Journal of Chemistry* 55 (2002): 381–398.

13. J. Norman, S. C. Moratti, A. T. Slark, D. J. Irvine, and A. T. Jackson, "Synthesis of Well-Defined Macromonomers by Sequential ATRP–Catalytic Chain Transfer and Copolymerization With Ethyl Acrylate," *Macromolecules* 35 (2002): 8954–8961.

14. T. P. Davis, D. M. Haddleton, and S. N. Richards, "Controlled Polymerization of Acrylates and Methacrylates 1," *Journal of Macromolecular Science, Part C: Polymer Reviews* 34, no. 2 (1994): 243–324.

15. M. Zhang and R. A. Hutchinson, "Synthesis and Utilization of Low Dispersity Acrylic Macromonomer as Dispersant for Nonaqueous Dispersion Polymerization," *Macromolecules* 51 (2018): 6267–6275.

16. G. W. Coates and M. Sawamoto, *Polymer Science: A Comprehensive Reference*, ed. M. Moeller and K. Matyjaszewski (Elsevier, 2012).

17. A. A. Gridnev and S. D. Ittel, "Catalytic Chain Transfer in Free-Radical Polymerizations," *Chemical Reviews* 101 (2001): 3611–3660.

18. T. P. Davis, D. Kukulj, D. M. Haddleton, and D. R. Maloney, "Cobalt-mediated Free-radical Polymerization of Acrylic Monomers," *Trends in Polymer Science* 3 (1995): 365–373.

19. J. Vandenbergh and T. Junkers, "Macromonomers From AGET Activation of Poly(*n*-Butyl Acrylate) Precursors: Radical Transfer Pathways and Midchain Radical Migration," *Macromolecules* 45 (2012): 6850–6856.

20. J. Vandenbergh and T. Junkers, "Synthesis of Macromonomers From High-Temperature Activation of Nitroxide Mediated Polymerization (NMP)-made Polyacrylates," *Macromolecules* 46 (2013): 3324–3331.

21. Y. Shen, S. Zhu, F. Zeng, and R. Pelton, "Versatile Initiators for Macromonomer Syntheses of Acrylates, Methacrylates, and Styrene by Atom Transfer Radical Polymerization," *Macromolecules* 33 (2000): 5399–5404.

22. F. Schön, M. Hartenstein, and A. H. E. Müller, "New Strategy for the Synthesis of Halogen-Free Acrylate Macromonomers by Atom Transfer Radical Polymerization," *Macromolecules* 34 (2001): 5394–5397.

23. A.-M. Zorn, T. Junkers, and C. Barner-Kowollik, "Synthesis of a Macromonomer Library from High-Temperature Acrylate Polymerization," *Macromolecular Rapid Communications* 30 (2009): 2028–2035.

24. M. F. Cunningham and R. A. Hutchinson, *Ch.7 of Handbook of Free Radical Polymerization*, vol. 1, ed. T. P. Davis and K. Matyjaszewski (John Wiley & Sons, Inc., 2002).

25. E. G. Bygott and R. A. Hutchinson, "The Use of High-Temperature Semi-Batch Radical Polymerization to Synthesize Acrylate Based Macromonomers and Structured Copolymers," *Macromolecular Chemistry and Physics* 225 (2024): 2300321.

26. N. Heidarzadeh, E. G. Bygott, and R. A. Hutchinson, "Exploiting Addition–Fragmentation Reactions to Produce Low Dispersity Poly(isobornyl acrylate) and Blocky Copolymers by Semibatch Radical Polymerization," *Macromolecular Rapid Communications* 41 (2020): 2000288.

27. N. Heidarzadeh and R. A. Hutchinson, "Maximizing Macromonomer Content Produced by Starved-Feed High Temperature Acrylate/Methacrylate Semi-Batch Polymerization," *Polymer Chemistry* 11 (2020): 2137–2146.

28. M. C. Grady, W. J. Simonsick, and R. A. Hutchinson, "Studies of Higher Temperature Polymerization of *n*-Butyl Methacrylate and M*n*-Butyl Acrylate," *Macromolecular Symposia* 182 (2002): 149–168.

29. A. N. F. Peck and R. A. Hutchinson, "Secondary Reactions in the High-Temperature Free Radical Polymerization of Butyl Acrylate," *Macromolecules* 37 (2004): 5944–5951.

30. F. S. Rantow, M. Soroush, M. C. Grady, and G. A. Kalfas, "Spontaneous Polymerization and Chain Microstructure Evolution in High-Temperature Solution Polymerization of *n*-Butyl Acrylate," *Polymer* 47 (2006): 1423–1435.

31. M. Hakim, V. Verhoeven, N. T. McManus, M. A. Dubé, and A. Penlidis, "High-temperature Solution Polymerization of Butyl Acrylate/Methyl Methacrylate: Reactivity Ratio Estimation," *Journal of Applied Polymer Science* 77 (2000): 602–609.

32. W. Wang and R. A. Hutchinson, "Free-radical Acrylic Polymerization Kineticsat Elevated Temperatures," *Chemical Engineering Technology* 33 (2010): 1745–1753.

33. C. Quan, M. Soroush, M. C. Grady, J. E. Hansen, and W. J. Simonsick, "High-Temperature Homopolymerization of Ethyl Acrylate Andn-Butyl Acrylate: Polymer Characterization," *Macromolecules* 38 (2005): 7619–7628.

34. T. Junkers and C. Barner-Kowollik, "The Role of Mid-Chain Radicals in Acrylate Free Radical Polymerization: Branching and Scission," *Journal of Polymer Science, Part A: Polymer Chemistry* 46 (2008): 7585–7605.

35. A. N. Nikitin and R. A. Hutchinson, "The Effect of Intramolecular Transfer to Polymer on Stationary Free Radical Polymerization of Alkyl Acrylates," *Macromolecules* 38 (2005): 1581–1590.

36. W. Wang, A. N. Nikitin, and R. A. Hutchinson, "Consideration of Macromonomer Reactions in *n*-Butyl Acrylate Free Radical Polymerization," *Macromolecular Rapid Communications* 30 (2009): 2022–2027.

37. J. P. A. Heuts and N. M. B. Smeets, "Catalytic Chain Transfer and Its Derived Macromonomers," *Polymer Chemistry* 2 (2011): 2407.

38. G. Nurumbetov, N. Engelis, J. Godfrey, et al., "Methacrylic Block Copolymers by Sulfur Free RAFT (SF RAFT) Free Radical Emulsion Polymerisation," *Polymer Chemistry* 8 (2017): 1084–1094.

39. B. Yamada, F. Oku, and T. Harada, "Substituted Propenyl End Groups as Reactive Intermediates in Radical Polymerization," *Journal of Polymer Science, Part A: Polymer Chemistry* 41 (2003): 645–654.

40. P. Cacioli, D. G. Hawthorne, R. L. Laslett, E. Rizzardo, and D. H. Solomon, "Copolymerization of ω-Unsaturated Oligo(Methyl Methacrylate): New Macromonomers," *Journal of Macromolecular Science: Part A - Chemistry* 23 (1986): 839–852.

41. B. Dervaux, T. Junkers, M. Schneider-Baumann, F. E. Du Prez, and C. Barner-Kowollik, "Propagation Rate Coefficients of Isobornyl Acrylate, *tert*-Butyl Acrylate and 1-Ethoxyethyl Acrylate: a High Frequency PLP-SEC Study," *Journal of Polymer Science, Part A: Polymer Chemistry* 47 (2009): 6641–6654.

42. N. M. Ahmad, F. Heatley, and P. A. Lovell, "Chain Transfer to Polymer in Free-Radical Solution Polymerization Ofn-Butyl Acrylate Studied by NMR Spectroscopy," *Macromolecules* 31 (1998): 2822–2827.

43. C. Plessis, G. Arzamendi, J. R. Leiza, H. A. S. Schoonbrood, D. Charmot, and J. M. Asua, "A Decrease in Effective Acrylate Propagation Rate Constants Caused by Intramolecular Chain Transfer," *Macromolecules* 33 (2000): 4–7.

44. A. N. Nikitin, R. A. Hutchinson, W. Wang, G. A. Kalfas, J. R. Richards, and C. Bruni, "Effect of Intramolecular Transfer to Polymer on Stationary Free-Radical Polymerization of Alkyl Acrylates, 5 – Consideration of Solution Polymerization up to High Temperatures," *Macromolecular Reaction Engineering* 4 (2010): 691–706.

45. W. Wang, R. A. Hutchinson, and M. C. Grady, "Study of Butyl Methacrylate Depropagation Behavior Using Batch Experiments in Combination With Modeling," *Industrial and Engineering Chemistry Research* 48 (2009): 4810–4816.

46. W. Wang and R. A. Hutchinson, "A Comprehensive Kinetic Model for High-Temperature Free Radical Production of Styrene/Methacrylate/Acrylate Resins," *AIChE Journal* 57 (2011): 227–238.

47. R. A. Hutchinson, D. A. Paquet, S. Beuermann, and J. H. McMinn, "Investigation of Methacrylate Free-Radical Depropagation Kinetics by Pulsed-Laser Polymerization," *Industrial and Engineering Chemistry Research* 37 (1998): 3567–3574.

48. B. Zdovc, H. Li, J. Zhao, D. Pahovnik, and E. Žagar, "Influence of Microstructure on the Elution Behavior of Gradient Copolymers in Different Modes of Liquid Interaction Chromatography," *Analytical Chemistry* 94 (2022): 7844–7852.

49. I. H. Alshehri, D. Pahovnik, E. Žagar, and D. A. Shipp, "Stepwise Gradient Copolymers Ofn-Butyl Acrylate and Isobornyl Acrylate by Emulsion RAFT Copolymerizations," *Macromolecules* 55 (2022): 391–400.

50. K. Philipps, T. Junkers, and J. J. Michels, "The Block Copolymer Shuffle in Size Exclusion Chromatography: The Intrinsic Problem With Using Elugrams to Determine Chain Extension Success," *Polymer Chemistry* 12 (2021): 2522–2531.

Supporting Information

Additional supporting information can be found online in the Supporting Information section.